

Research Article

A Comparative Analysis of PID, Lead, Lag, Lead-Lag, and Cascaded Lead Controllers for a Drug Infusion System

Zuwwar Khan Jadoon, Sobia Shakeel, Abeera Saleem, Ali Khaqan, Sana Shuja, Qadeer ul-Hasan, Shahzad A. Malik, and Raja Ali Riaz

Department of Electrical Engineering, COMSATS Institute of Information Technology, Chak Shahzad Park Road, Islamabad, Pakistan

Correspondence should be addressed to Ali Khaqan; ali_khaqan@comsats.edu.pk

Received 23 February 2017; Revised 26 July 2017; Accepted 7 August 2017; Published 20 September 2017

Academic Editor: Maria Lindén

Copyright © 2017 Zuwwar Khan Jadoon et al. This is an open access article distributed under the Creative Commons Attribution License, which permits unrestricted use, distribution, and reproduction in any medium, provided the original work is properly cited.

Goal. The aim of this paper is to conduct a comprehensive comparative analysis between five different controllers for a drug infusion system in total intravenous anesthesia (TIVA) administration. **Methods.** The proposed method models a dilution chamber with first order exponential decay characteristics to represent the pharmacokinetic decay of a drug. The dilution chamber is integrated with five different control techniques with a simulation-based comparative analysis performed between them. The design process is conducted using MATLAB SISOTOOL. **Results.** The findings show that each controller has its own merits and demerits. The results generated using MATLAB signify and confirm the effectiveness of PI and cascaded lead controllers, with cascaded lead controller as the best control technique to automate and control the propofol delivery. **Conclusion.** In this paper, different control techniques for measurement-based feedback-controlled propofol delivery is confirmed with promising results. **Significance.** The comparative analysis showed that this drug infusion platform, merged with the proper control technique, will perform eminently in the field of total intravenous anesthesia.

1. Introduction

In the field of general anesthesia, target-controlled infusion of anesthesia (TCIA) is a well-recognized technique, found among the most widely recognized closed-loop drug delivery methods [1–3]. Anesthetic drug administration in the human body is a cynosure for the researchers, requiring cardinal attention in the field of biomedical engineering. A paucity or surfeit amount of dose could lead the patient in a precarious condition such as intoxication. Propofol is a nonopioid anesthetic agent, which is widely used for intravenous administration in the field of general anesthesia. Therefore, due to its extensive use and legion advantages, it is exacting to achieve and maintain its target concentration [4, 5].

Pharmacokinetics (PK) is a branch of pharmacology that is related to the study of how a living organism affects the infused drug, while pharmacodynamics (PD) is the branch of pharmacology that is concerned with the study of how

the infused drug affects a living organism. Considering all the important parameters, precise pharmacokinetic (PK) and pharmacodynamic (PD) models are developed, on the basis of which TCIA is introduced. The efficacy of TCIA depends on the precision of the PK model, the mutual relation between the effect site concentration and measurement, and the device used for drug monitoring and control. To achieve radical control over the drug delivery, continuous propofol measurement is performed throughout total intravenous anesthesia (TIVA).

In [6, 7], a canonical three-compartmental model has been used to describe the qualities and peculiarities of drug concentration and dynamical mobility inside the human circulatory system. The first compartment constitutes the volume of blood, where drug is injected. After the drug delivery, the drug concentration in different individual compartments including the effect site, that is, the brain, is impacted due to various factors. These factors include

distribution rate constants within interacting compartments, volume comprising the respective compartments and rate of the drug infusion.

Setting the drug concentration degree at the effect site to the desired targeted degree is precisely the main goal of TCIA. The drug is infused and measured in the blood that is the first compartment. In such case, by using the pharmacodynamic models, measurement of drug concentration in the blood provides an estimation of effect site drug concentration. Once the drug concentration is quantified in the blood, its control and regulation to a desired targeted level can also be accomplished.

In a closed-loop drug delivery system, different control techniques are employed in order to control the drug infusion rate, which leads to the control of drug concentration in the blood and therefore at the effect site. In [8–11], PID controllers are discussed as being the simplest controllers, which are widely used in the field of control system design. References [12, 13] discuss vulnerability to high-frequency noise and integrator windup effect as one of the main disadvantages of a PID controller. The most viable alternatives are lead, lag, or an adjustment of both controllers, where design parameters are available, studied in [14, 15]. In some cases, discussed in [16, 17], second order lead and lag controllers, compared with the widely used PID controllers, lead to better results.

The phase lead and phase lag are two of the most commonly utilized control architectures for designing control systems with the root locus or bode compensation approach used. In [18], the cascade or series compensation is stated as the most popular method in the control system design. The design and implementation of lead and lag controllers have been studied in [19–22]. A conceptual understanding in control system engineering is provided in [23]. A comparative analysis of different control techniques is studied in [24, 25].

This paper focuses on the comparative analysis of five different control techniques and their design process, to automate the delivery of an infusion system, based on propofol measurement in a closed-loop feedback system. The comparative analysis is conducted with respect to different time domain specifications like gain, percentage overshoot, settling time, and rise time. The design process of phase-lead, lag, lead-lag, and cascaded lead controllers is performed by applying the principles of the root locus technique [26–28], using MATLAB SISOTOOL [29–31]. The simulation study is based on the model developed by Myers et al. in [32].

This paper is organized as follows: Section 2 describes the system modeling and its description. Section 3 presents the methods employed in an open-loop and closed-loop analysis. Section 4 shows the simulation results for five different controllers, and the comparative analysis has been drawn on the basis of different parameters for example rise time, overshoot, and settling time. Section 5 comments on the discussion of the paper. Finally, Section 6 concludes the paper.

2. System Model and Description

The following equations, as shown by Myers et al. in [32], are used in system modeling.

After the introduction of a bolus injection or propofol infusion, a first-order kinetics model depicts the drug elimination dynamics in blood circulation, mathematically described as

$$\frac{dC(t)}{dt} = -\lambda C(t). \quad (1)$$

The model represents an exponential decay in drug concentration over time

$$C(t) = C(t_0)e^{-\lambda t}, \quad (2)$$

where $C(t)$ represents the time-dependent drug concentration and $C(t_0)$ describes the concentration of drug at time, $t = t_0$. λ represents the drug elimination rate which is a function of the volume of the blood and PK decay rate.

When the drug is injected in the blood at an infusion rate $i(t)$, (1) is qualified as

$$\frac{dC(t)}{dt} = -\lambda C(t) + \frac{i(t)}{V}. \quad (3)$$

In our simulation study, a dilution chamber of constant volume is used to mimic the human blood. The exponential decay of drug concentration in this chamber models the actual PK decay of the drug in the blood. The drug elimination rate λ is determined as

$$\lambda = \frac{\Omega}{V_1}. \quad (4)$$

V_1 shows the volume of the chamber and Ω represents the dilution flow rate.

A particular amount of drug injection increases the concentration level inside the chamber. This new concentration of the chamber is defined as initial concentration, that is, $C_1(0)$, which decays exponentially over time. The decaying exponential rate is set by Ω and V_1

$$C_1(t) = C_1(0)e^{-(\Omega/V_1)t}. \quad (5)$$

The dynamics of concentration in the dilution chamber can equally be symbolized in the derivative form as

$$\frac{dC_1(t)}{dt} = -\frac{\Omega}{V_1}C_1(t). \quad (6)$$

The bolus dose, when merged with continuous infusion results in the time-dependent concentration, changes in the dilution chamber as

$$\frac{dC_1(t)}{dt} = -\frac{\Omega}{V_1}C_1(t) + \frac{i(t)}{V_1}. \quad (7)$$

The system model in terms of its differential equation is represented by (7).

Figure 1 shows the block diagram of the feedback-controlled drug infusion system. It is comprised of the following:

- (1) A controller to achieve the target concentration of propofol

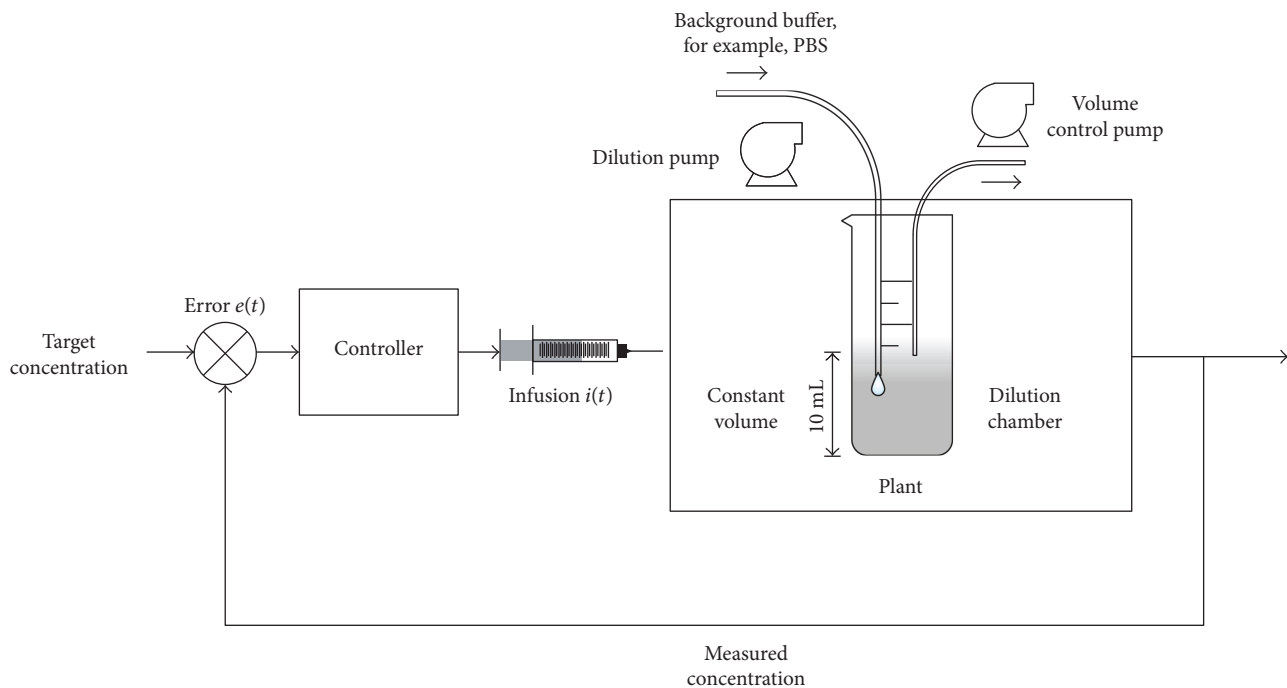


FIGURE 1: Block diagram of a feedback-controlled drug infusion system.

- (2) A constant volume dilution chamber, representing the first compartment, which is our plant
- (3) A dilution pump to regulate the continuous dilution rate of the background electrolyte
- (4) A volume control pump to maintain a constant volume in the chamber.

3. Methods

To analyze the performance of the feedback-controlled drug infusion system, a dilution chamber with constant volume V_1 is considered. In order to vary the initial concentration $C_1(0)$ over time, the dilution chamber is diluted continuously by a background electrolyte via a dilution pump at a dilution rate (Ω). The concentration change from an initial concentration inside the dilution chamber is described in (3). At first, the system is analyzed in an open loop, following the closed-loop system design and implementation, using five different control schemes.

3.1. Open-Loop Analysis. The open-loop analysis can be described by the following two steps. The first step describes the exponential decay of the dilution chamber. V_1 describing the volume of the chamber is fixed at 10 mL. $C_1(0)$ describing the initial concentration of the propofol was set to 0.01 mL. In order to mimic the PK decay, this initial concentration is diluted by the continuous dilution of a background electrolyte at a flow rate of 0.04 mL/s.

In the second step, the same volume is maintained in the dilution chamber, that is, 10 mL; however, the concentration of propofol in the chamber is set to zero, that is,

TABLE 1: Simulation parameters.

Variable	Description	Value
$i(t)$	Infusion rate	Controller calculated infusion rate
$C_1(t)$	Concentration of the dilution chamber	Time dependent
Target	Target concentration of the dilution chamber	0.038 mMol
V_1	Volume of the dilution chamber	10 mL
Ω	Speed of dilution pump/dilution flow rate	0.04 mL/s
λ	Elimination rate $\lambda = \Omega/V_1$	0.004 s^{-1}

$C_1(0) = 0$. Afterwards, both continuous dilution and propofol infusion are processed in a parallel operation with a fixed infusion rate.

The design parameters of the open-loop analysis are shown in Table 1. Figure 2 shows the open-loop step response of the uncontrolled system with a very high settling time, rise time, and steady state error. However, the overshoot percentage in the system response is almost zero.

3.2. Control Techniques and Designs. This section presents the closed-loop design analysis of the drug infusion system. In order to achieve the target-controlled drug infusion in the first compartment or the dilution chamber, five different control techniques are designed and implemented in a closed-loop feedback system. The fundamentals of the techniques employed in the meticulous design process of all five dynamic controllers are referred to [33–35]. The design techniques described in the closed-loop analysis of

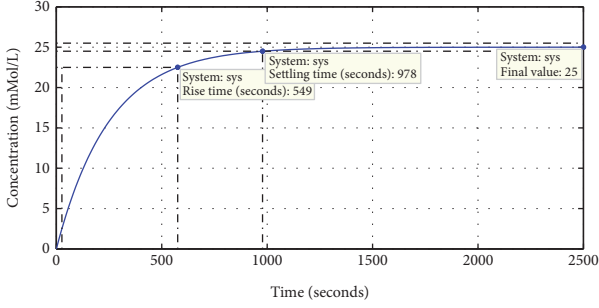


FIGURE 2: Step response of the uncontrolled dilution chamber.

TABLE 2: Effects of K_p , K_D , and K_I in a PID controller.

Response	Rise time	Overshoot	Settling time	Steady state error
K_p	Decrease	Increase	No effect	Decrease
K_I	Decrease	Increase	Increase	Eliminate
K_D	No effect	Decrease	Decrease	No effect

the infusion system uses the same parameters as have been used in the open-loop analysis. The design parameters are shown in Table 1.

3.2.1. PID Controller. The proportional-integral-derivative (PID) controller is one of the most commonly used and universally accepted control algorithm used in control industry. The PID controller is popular for its attributes partly to their wide-range operation of robust performance and partly to their simplified operation. The term PID describes its three main components, a proportional control term (K_p), an integral control term (K_I), and a differential control term (K_D). Table 2 describes the effect of a PID controller in terms of its three components. Mathematically, the following equations describe a PID controller:

$$e(t) = \text{target} - \mathbb{C}(t), \quad (8)$$

$$i(t) = K_p e(t) + K_I \int_0^t e(t) dt + K_D \frac{de(t)}{dt}. \quad (9)$$

By keeping the same parameters, as used in the open-loop analysis, a PID controller is designed to yield the targeted concentration. In the study, conducted by Myers et al. in [32], a PID controller is triggered after the bolus injection is injected. A minor amount of fluctuation in drug concentration is observed. Therefore, K_D part of the controller is set to zero. By connecting the PI controller with the dilution chamber in a closed-loop system, nine runs are recorded for each of the nine parameters in Table 3. Finally, the PI controller is tuned by using parameter 5 to control the closed-loop drug delivery. The parameter set employed in our simulation study is identified from the experimental and simulation parameters in [32].

The open-loop dynamics plus the system modeling represented in (7) and the mathematical description of the PID controller in (8) and (9) collectively present a complete

TABLE 3: PI parameters.

PI parameters	K_p	K_I
1	3,000,000	55
2	6,000,000	55
3	750,000	55
4	4,500,000	5.5
5	4,500,000	55
6	4,500,000	550
7	4,500,000	5500
8	4,500,000	55,000
9	4,500,000	550,000

picture of the closed-loop flow system. A PID controller, incorporated with the dilution chamber in a closed-loop feedback system, is illustrated in Figure 3. By tuning the PI controller using parameter 5, that is, $K_p = 4.5 \times 10^6$ and $K_I = 55$, the closed-loop transfer function of the PI-controlled dilution chamber is obtained as

$$G_{CL}(s) = \frac{4,500,000s + 55}{10s^2 + 4,500,000s + 55}. \quad (10)$$

3.2.2. Phase-Lag Controller. By adding equal numbers of poles and zeros, a phase-lag controller provides an appreciable amount of relative stability to a system, yielding slow response time. In a phase-lag controller, the pole of the controller is placed closer to the origin as compared to the zero of the controller. The generalized transfer function of a phase-lag controller is given as

$$C(s) = \frac{s+z}{s+p}, \quad (11)$$

where

$$p < z. \quad (12)$$

To address the steady state error, a phase-lag controller is designed, using the root locus method. The target is to achieve a compensated steady state error value of $E_{ss} < 0.01$, without affecting the transients, where E_{ss} represents the compensated steady state error. In case of a lag controller, varying the transients leads to slower response time [35], which is not desired. The phase-lag controller is designed using the following two steps.

In the first step, the z/p ratio is evaluated. Suppose we have a system $G(s)$, incorporated with a lag controller $C(s) = (s-z)/(s-p)$.

Using the final value theorem [36], first, a formula for steady state error (final value of the error) is calculated

$$E_{ss} = \lim_{s \rightarrow 0} s \cdot \frac{U(s)}{1 + (G_N(s)/G_D(s)) \cdot ((s-z)/(s-p))}. \quad (13)$$

For step input, $U(s) = 1/s$, the above equation, after applying the limit, simplifies to

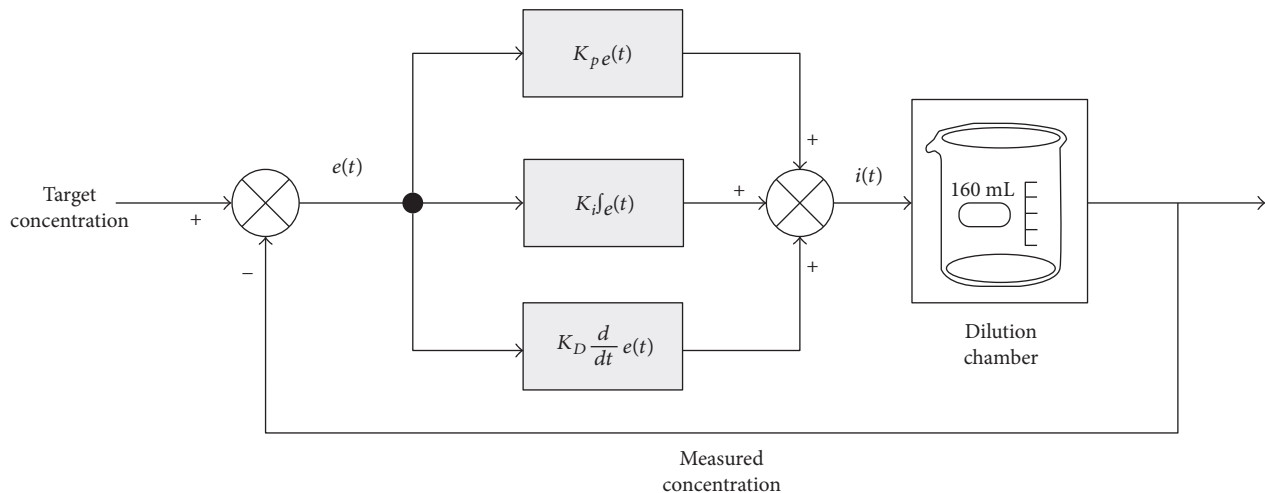


FIGURE 3: Block diagram of a PID controller connected with the dilution chamber in a closed-loop feedback system.

$$E_{ss} = \frac{G_D(0) \cdot p}{G_D(0) \cdot p + G_N(0) \cdot z}. \quad (14)$$

Now, by solving for the ratio of the zero to the pole, we get the following final equation:

$$\frac{z}{p} = \frac{G_D(0) - E_{ss} G_D(0)}{E_{ss} G_N(0)}, \quad (15)$$

where z and p represent the zero and pole of the controller, while $G_D(0)$ and $G_N(0)$ are the denominator and numerator of the system transfer function $G(s)$ at $s \rightarrow 0$.

In the second step, the location of the zero and pole of the controller is determined using an algebraic approach. In order for a point P to exist on the root locus, the sum of the angles of all the poles minus the sum of the angles of all the zeros has to equal 180° [36]. The angle stated corresponds to the angle of the line from the open-loop pole or zero to that from point P on the root locus. Figure 4(a) graphically explains the above concept of root locus existence by considering a second-order pseudo system S .

Mathematically,

$$\sum \theta_p - \sum \theta_z = 180^\circ. \quad (16)$$

Now, to delineate the pole zero placement (design process) of the *actual* phase-lag controller, the same second-order pseudo system S is considered and incorporated with a pseudo phase-lag controller C . Figure 4(b) shows the changed root locus and a considerable amount of root locus shaping of the system S , when merged with controller C . Following the concept of the root locus existence from (16),

$$\theta_1 + \theta_2 + \theta_p - \theta_z = 180^\circ, \quad (17)$$

where θ_1 and θ_2 are the angles associated with the poles of the pseudo system S and θ_p and θ_z are the angles associated with the pole and zero of the pseudo lag controller C . Now, in order to have no root locus shaping, the angle contribution

of both the pole and zero of the controller C should be close to zero, as shown in Figure 4(c) Mathematically,

$$\theta_p - \theta_z \approx 0. \quad (18)$$

Now, considering the *actual* system, that is, the dilution chamber, to achieve the above two requirements of negligible angle difference and minimum root locus shaping as shown in (18) and Figure 4(c), respectively, the following procedure is implemented. The pole and zero of the actual phase-lag controller are placed closer to each other and to the origin with the same z/p ratio as calculated in the first step using (15). By doing such placement, the angles for the pole and zero became closer and closer together and the requirement in (18) is met. Pole zero placement of the controller is found using (19) and (20). The gain (k), required to achieve the desired steady state error, is computed using MATLAB SISOTOOL.

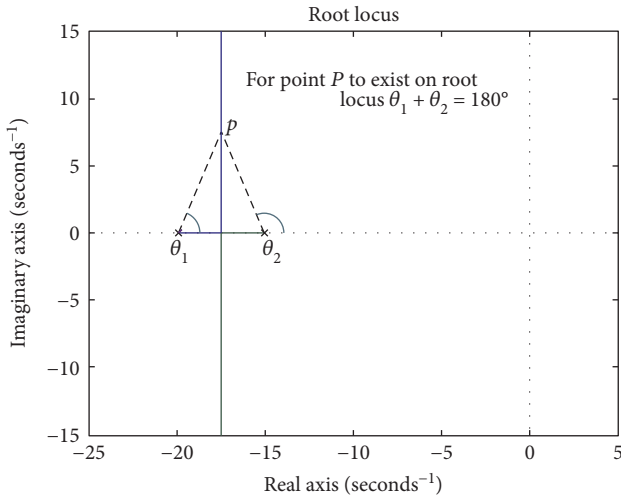
$$z = \frac{\text{real closed-loop dominant pole}}{50}, \quad (19)$$

$$p = \frac{z}{z/p}. \quad (20)$$

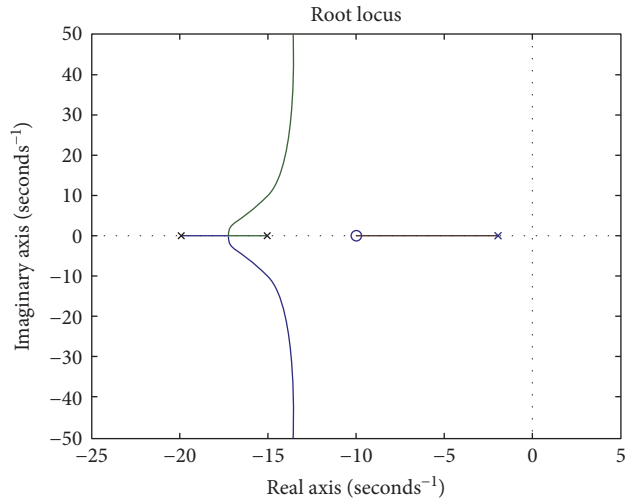
The appropriate placement and zero-angle contribution ($\theta_p - \theta_z \approx 0$) of the pole and zero of the controller is shown in Figure 5, verifying no root locus shaping. The bottom line of the steps involved in the whole designing process is stated as the following:

- (1) The z/p ratio is maintained, which is needed for the compensated steady state error (E_{ss}).
- (2) The z and p of the lag controller are kept as close to the imaginary axis as possible to avoid shaping the root locus and the transients.

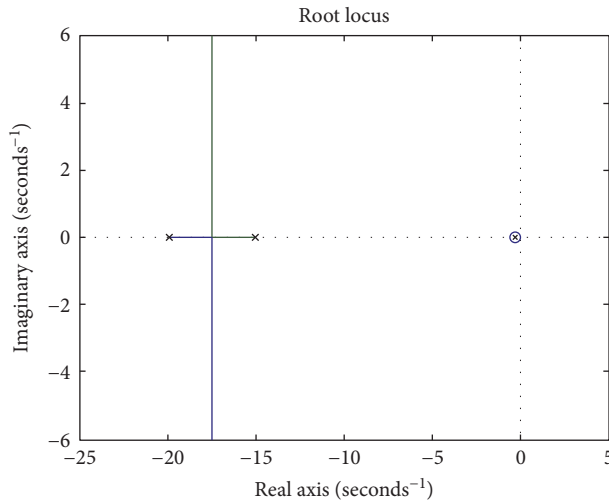
The design details of the phase-lag controller are illustrated in Figure 6. The transfer function of the designed phase-lag controller with adjusted gain $k = 30$ is



(a) Root locus existence using two poles of a system S



(b) Pole zero placement using system S and controller C with root locus shaping



(c) Pole zero placement using system S and controller C with no root locus shaping

FIGURE 4: Graphical illustration of root locus existence shaping and the concept of pole zero placement using a pseudo system S and a pseudo lag controller C .

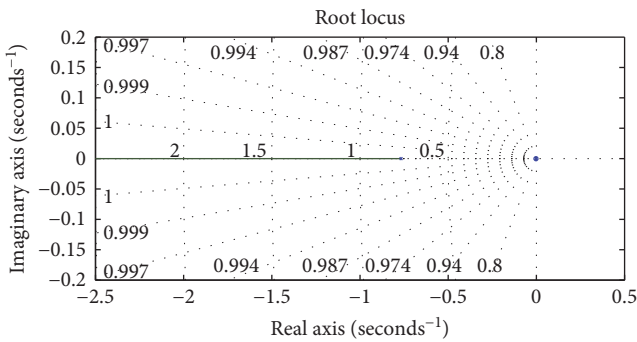


FIGURE 5: Root locus of the system incorporated with the designed lag controller.

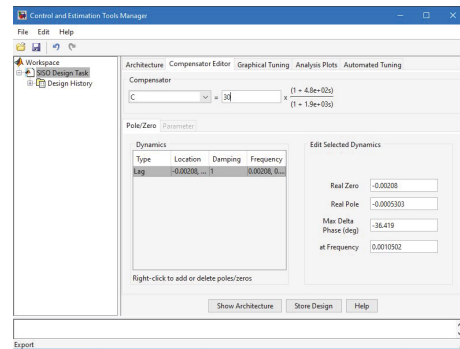


FIGURE 6: Illustration of the design details of the phase-lag controller.

$$G_c(s) = \frac{7.5757(s + 0.0021)}{s + 0.0005303}. \quad (21)$$

The controller, when merged with the dilution chamber, resulted in the following closed-loop transfer function

$$G_{CL}(s) = \frac{0.75757(s + 0.0021)}{(s + 0.002096)(s + 0.76)}. \quad (22)$$

3.2.3. Phase-Lead Controller. By adding equal numbers of poles and zeros, a phase-lead controller provides an appreciable improvement in the transient response of a system, increasing the open-loop gain in some cases. Increasing gain leads to more susceptibility to noise. In case of a lead controller, the zero of the controller is placed closer to the origin as compared to the pole of the controller. The generalized transfer function of a phase-lead controller is given as

$$C(s) = \frac{s + z}{s + p}, \quad (23)$$

where

$$p > z. \quad (24)$$

To achieve a faster response time, a phase-lead controller is designed, using the root locus method. In a root locus plot, the location where the asymptotes cross the real line is called the center of gravity or the centroid, defined in (15). A lead controller shifts the root locus towards the left side of the s -plane by shifting the centroid, the asymptotes, and the closed-loop poles to the left, thus providing a faster response [36]. Figures 7(a) and 7(b) graphically illustrates the effects of a phase-lead controller in terms of centroid movement and root locus shaping by considering a second-order pseudo system S and a pseudo phase-lead controller C .

$$\text{Centroid} = \frac{\sum \text{finite poles} - \sum \text{finite zeros}}{n - m}, \quad (25)$$

where n = number of poles and m = number of zeros.

Now, to achieve the desired output, the actual phase-lead controller is designed using the following steps:

- (1) The zero of the controller is kept near the imaginary axis, as compared to the pole of the controller.
- (2) The pole of the controller is kept far from both the zero of the controller and the imaginary axis.
- (3) The distance between the pole and the zero of the controller is kept large.
- (4) The added pole has a larger negative value than the added zero, as zero resides near the origin.

The design details of the phase-lead controller are illustrated in Figure 8. The transfer function of the designed phase-lead controller with gain $k = 500$ is given as

$$G_c(s) = \frac{10,000(s + 10)}{s + 200}. \quad (26)$$

The designed phase-lead controller and the dilution chamber in a closed-loop system, resulted in the following transfer function:

$$G_{CL}(s) = \frac{1000(s + 10)}{(s + 8.393)(s + 1192)}. \quad (27)$$

3.2.4. Phase-Lead-Lag Controller. Both phase-lead and lag controllers have their own advantages and disadvantages as discussed above. Practical systems often demand certain rigorous specifications, where a combination of both lead and lag controllers can be practicable. The generalized transfer function of a phase-lead-lag controller is

$$C(s) = \frac{a_1 \tau_1 s + 1}{\tau_1 s + 1} \cdot \frac{a_2 \tau_2 s + 1}{\tau_2 s + 1}, \quad (28)$$

where

$$a_1 > 1, a_2 < 1. \quad (29)$$

To attain both faster response and relative stability, a phase-lead-lag controller is designed using the same design principles as have been discussed in the phase-lead and phase-lag sections. The following two steps describe the whole design process.

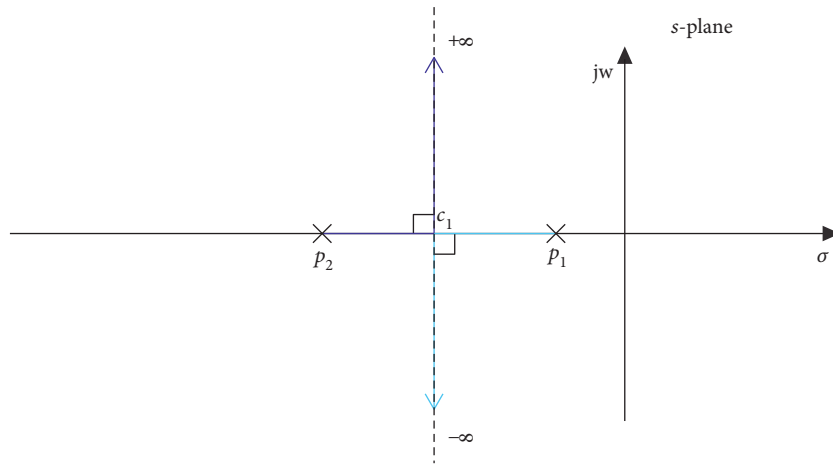
In the first step, a phase-lead controller is designed using the following procedure:

- (1) The pole of the controller is placed farther into the left half plane away from the imaginary axis.
- (2) The zero of the controller is placed near the imaginary axis.
- (3) The pole and zero of the controller are placed at such points, so that the distance between them is large enough and the centroid is shifted further to the left half plane.

In the second step, a phase-lag controller is designed with a different approach due to the succeeding reason. In a traditional lag controller design, the main target is to eliminate steady state error without varying the transients and root locus shaping. Instead of implementing the conventional approach, here, the main target is to achieve *both* elimination of steady state error as well as a fast response. For such requirement, varying the transients and root locus shaping is needed, which is accomplished in a different way, described as following:

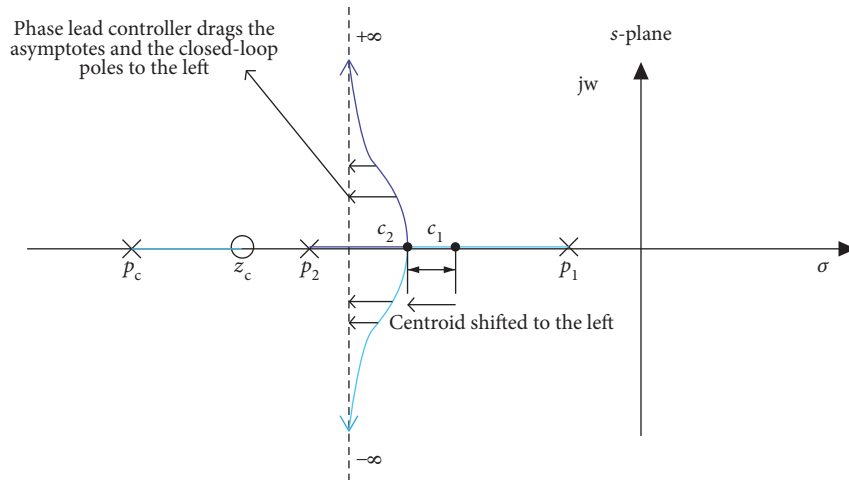
- (1) Unlike the traditional pole zero placement of a lag controller, zero of the controller is placed away from both the pole of the controller and the imaginary axis.
- (2) Unlike in (18), $\theta_p - \theta_z$ is kept greater than 0, instead of closer to 0, where θ_p and θ_z are the angles associated with the pole and zero of the controller, respectively.

A small amount of root locus shaping due to $\theta_p - \theta_z \neq 0$ is verified and illustrated in Figure 9.



*p*₁ System pole
*p*₂ System pole
*z*_c Controller zero
*c*₁ Centroid before adding lead controller
*c*₂ Centroid after adding lead controller

(a) Root locus of the pseudo system S without a pseudo lead controller C



*p*₁ System pole
*p*₂ System pole
*z*_c Controller zero
*c*₁ Centroid before adding lead controller
*c*₂ Centroid after adding lead controller

(b) Root locus of the pseudo system S with a pseudo lead controller C

FIGURE 7: Graphical illustration of effects of a phase-lead controller on root locus using a pseudo system S and a pseudo lead controller C.

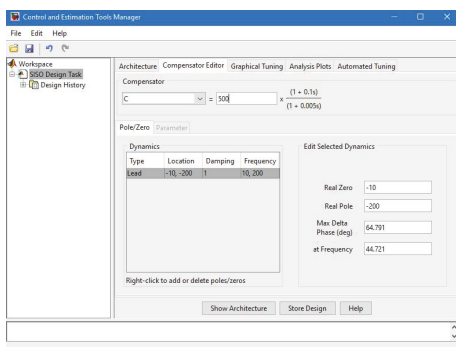


FIGURE 8: Illustration of the design details of the phase-lead controller.

The design details of the phase-lead-lag controller are illustrated in Figure 10. The transfer function of the designed lead-lag controller with gain, $k=500$ results as follows:

$$G_c(s) = \frac{4094.7(s + 7.29)(s + 10)}{(s + 3.98)(s + 150)}. \quad (30)$$

The controller when incorporated with the dilution chamber resulted in the following closed-loop transfer function:

$$G_{CL}(s) = \frac{409.47(s + 7.29)(s + 10)}{(s + 549.6)(s^2 + 13.87s + 54.32)}. \quad (31)$$

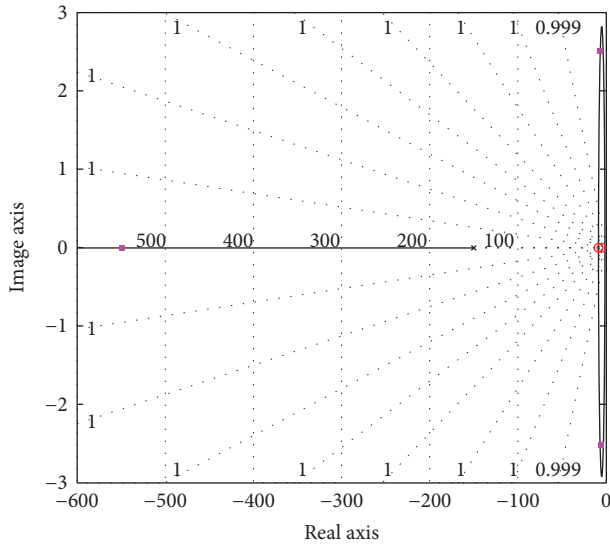


FIGURE 9: Root locus of the system incorporated with the designed lead lag controller.

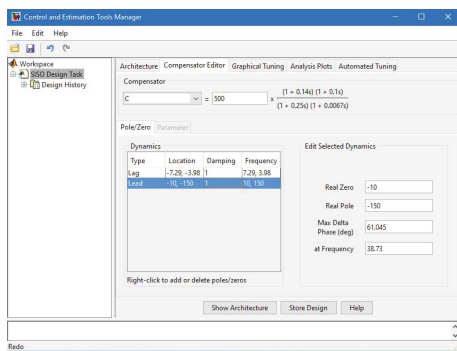


FIGURE 10: Illustration of the design details of the phase-lead lag controller.

3.2.5. *Cascaded Lead Controller.* Generally, a cascaded phase-lead controller is applied to attain a very fast response time. Applying two lead controllers in series, merged with the plant in a closed-loop feedback system, can significantly accelerate the system response time. In case of a drug infusion system, a faster response is required because a small delay or overshoot in drug delivery can lead to severe consequences. The transfer function of a traditional cascaded lead controller is

$$C(s) = \frac{s + z_1}{s + p_2} \cdot \frac{s + z_2}{s + p_1}, \quad (32)$$

where

$$p_1 > z_1, p_2 > z_2. \quad (33)$$

To achieve a much higher response time, a cascaded phase-lead controller is designed. The design principles are similar to what has been discussed in the phase-lead section. To achieve maximum desired output, consider the following:

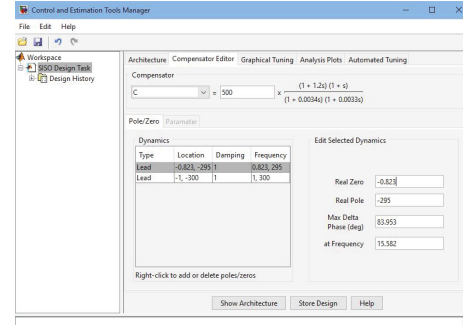


FIGURE 11: Illustration of the design details of the cascaded lead controller.

- (1) Both poles of the two lead controllers are placed farther from the imaginary axis into the left half plane.
- (2) Both zeros of the two lead controllers are placed near the imaginary axis.
- (3) Maximum distance between the poles (p_1, p_2) and zeros (z_1, z_2) of the two lead controllers is kept.

Mathematically,

$$\begin{aligned} p_1 - z_1 &\gg \text{average distance,} \\ p_2 - z_2 &\gg \text{average distance,} \end{aligned} \quad (34)$$

where p_1 and p_2 represent the poles and z_1 and z_2 represent the zeros of the two cascaded lead controllers.

The design details of the cascaded lead controller are illustrated in Figure 11. The transfer function of the designed cascaded phase-lead controller with gain $k = 500$ is

$$G_c(s) = \frac{5.3767 \times 10^7 (s + 0.823)(s + 1)}{(s + 295)(s + 300)}. \quad (35)$$

The designed cascaded phase-lead controller, when incorporated with the drug infusion system, resulted in the following closed-loop transfer function:

$$G_{CL}(s) = \frac{5.3767 \times 10^6 (s + 1)(s + 0.823)}{(s + 5.377 \times 10^6)(s + 1.07)(s + 0.7688)}. \quad (36)$$

4. Results

4.1. *Open-Loop Results.* To understand the first-order exponential decay of the dilution chamber, open-loop characteristics of the system were assessed in two steps in Section 2 of the open-loop analysis. The first step describes the dilution chamber in terms of its exponential decay property. The initial concentration of the propofol was set to 0.01 mMol/L in a fixed 10 mL volume of the dilution chamber. The result in Figure 12 shows and substantiates an exponential decay of concentration over time in the dilution chamber, due to the continuous dilution of the background electrolyte. The resultant plot is in perfect agreement with the theoretical computations using (4) and (5)

$$C_1(t) = 0.01e^{-0.004t}. \quad (37)$$

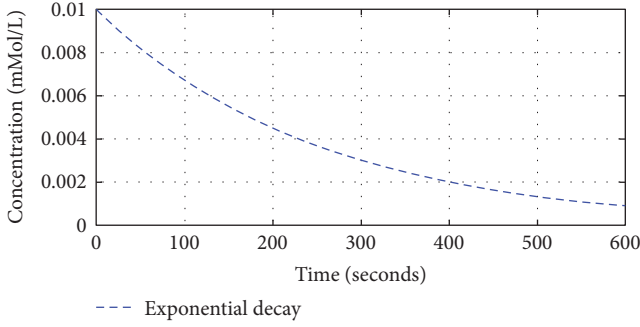


FIGURE 12: Exponential decay in concentration with propofol concentration = 0.01 mM and dilution flow rate = 0.04 mL/s.

In the second step, identification and validation of the open-loop gain and steady state analysis of the system is performed. Theoretically, the steady state gain is calculated from (7) in the system model and description. At steady-state $dC_1(t)/dt$ goes to zero, and the open-loop gain G of the system will be

$$G = \frac{C_1(t)}{i(t)} = \frac{1}{\lambda V_1} = \frac{1}{\Omega} = 25 \text{ s/mL}. \quad (38)$$

Propofol infusion, in parallel with the continuous dilution, is carried out for a certain duration. After some time, an equilibration state is achieved between the infusion and elimination rate of propofol. At such point, $dC_1(t)/dt$ goes to zero and the concentration level approaches its steady state.

The above infusion-dilution equilibrium led to the succeeding conception. For a particular value of dilution flow rate, a defined infusion rate results into a specific steady state concentration point. For a dilution flow rate of 0.04 mL/s, at five different infusion rates, the open-loop gain and the corresponding steady state concentration is evaluated and illustrated in Figure 13. The theoretical values calculated from (38) for different infusion rates completely meet the linear ratio as illustrated.

4.2. Closed-Loop Results. Five different control schemes were employed in order to achieve the target drug concentration in a closed-loop feedback system. The PI controller was tuned with nine different parameters, shown in Table 3, with various parameters showing closer results to each other leading to overlapping response time, as shown in Figure 14(a). The effectiveness of K_p and K_I can be depicted from the graph in the following manner. The proportional term K_p corresponds to the high rise time and settling time while the integral term K_I corresponds to an improved final value of the response. The PI controller, when tuned with the fifth parameter in Table 3, yields a more effective response time in comparison with other nine parameters, as shown in Figure 14(b).

Figure 14(c) illustrates the comparison between a phase-lag, lead, and lead-lag controllers when incorporated with the dilution chamber in a closed loop. The phase-lag controller significantly improves the steady state error of the system,

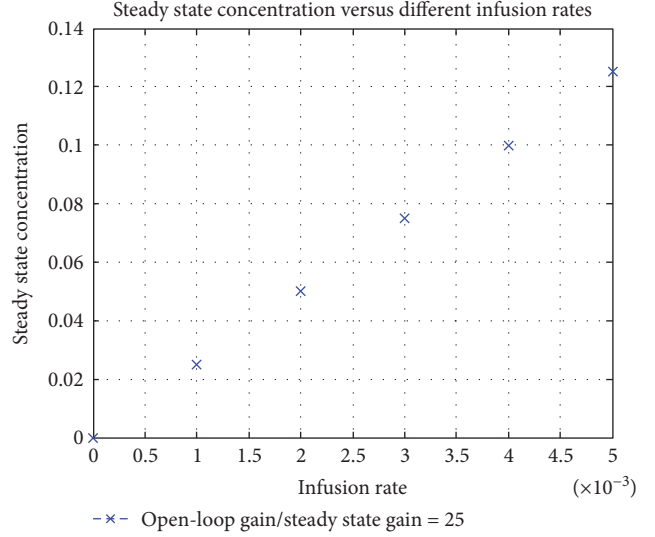


FIGURE 13: Steady state concentration at five different infusion rates with a flow rate, $\Omega = 0.04$ mL/s.

when compared with the open-loop step response in Figure 2: however, it does not contribute much to the response time as required. The phase-lead controller provides a much faster response as compared to a phase-lag controller as expected but still does not meet the higher response time requirements. The phase-lead-lag controller provides *both* faster response and steady state error reduction and therefore meets the objective as desired in the phase-lead-lag section of Section 3. The response time using a lead-lag controller seems closer to a single lead controller but better than a single lag controller.

Figure 15(a) shows the response time of the system when incorporated with a cascaded lead controller in a closed-loop feedback system. Due to two lead controllers in series and effective pole zero placement, the response time is much faster as compared to all the other control techniques discussed above.

Figure 15(b) shows the comparative analysis between the closed-loop results using PI and cascaded lead controller. The PI controller and cascaded lead controller both result into a much faster and stable response as compared to other controllers; however, the cascaded lead controller shows relatively better results than the PI controller. Table 4 scrutinizes the pros and cons of all five controllers in terms of the different time domain characteristics for each control technique.

5. Discussion

To target and maintain the drug concentration level in the human body, represented by a dilution chamber, five different control schemes are designed and implemented with a simulation-based comparative analysis between each of them. The comparative simulation study elucidates the effectiveness of each controller in targeting and maintaining the propofol level.

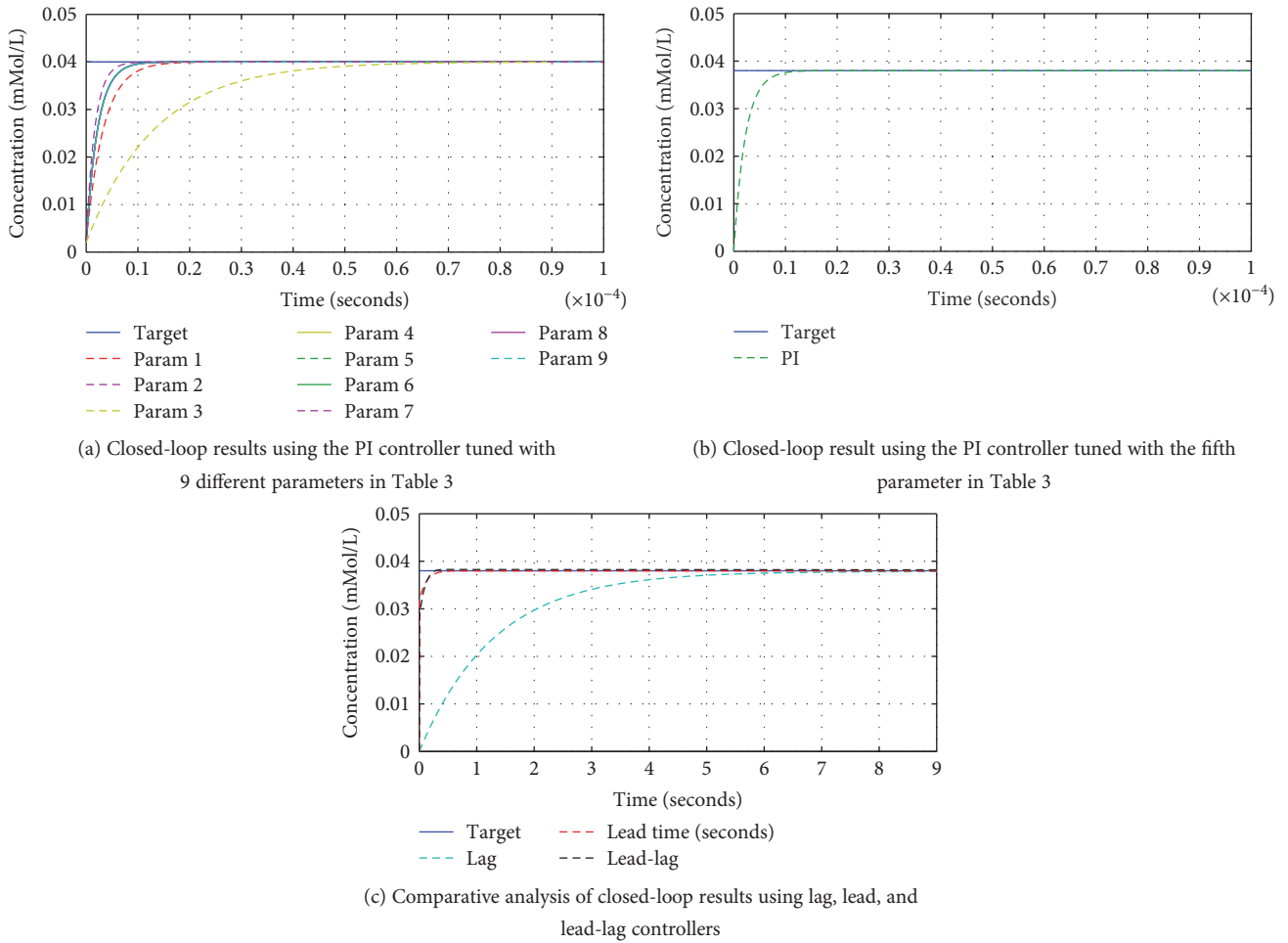


FIGURE 14: Comparative analysis of closed-loop results using PI, lead, lag, and lead-lag controllers.

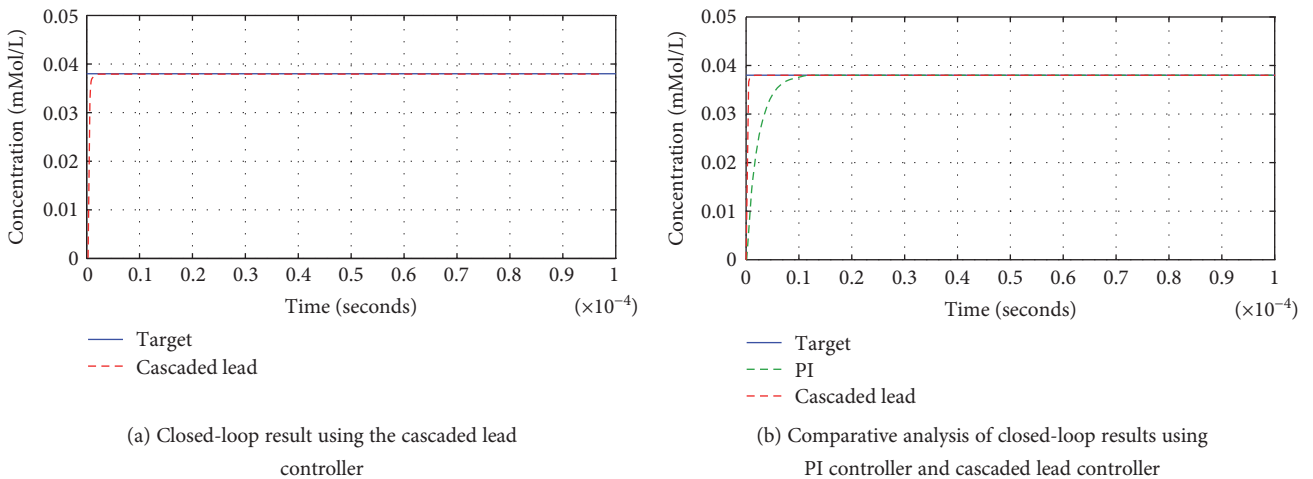


FIGURE 15: Comparative analysis of closed-loop results using cascaded lead controller and PI controller.

The drug concentration and dynamics are represented using the constant volume dilution chamber, due to the succeeding two *phenomena*. These are exponential decay of drug concentration in the dilution chamber and the steady state

analysis of the system, explained thoroughly in step 1 and step 2 of the open-loop analysis, in Section 3. The open-loop results in Section 4 also gives a concrete substantiation of both *phenomena*.

TABLE 4: Controller performance characteristics (a comparative analysis).

Controller	Gain	Rise time (sec)	Settling time (sec)	Overshoot (%)
Lag	30	2.9120	5.2720	0
Lead	500	0.0573	0.2492	0
Lead-lag	500	0.0880	0.1980	0.7164
PI	4.5×10^6	4.8822×10^{-6}	8.6935×10^{-6}	0
Cascaded lead	500	4.0862×10^{-7}	7.2779×10^{-7}	0

In our *simulation-based study*, the results shown using a PI controller incorporated with the dilution chamber demonstrate a fast response time with a negligible amount of overshoot and no steady state error percentage. However, the results generated by Myers et al., using the same PI controller, showed a fast response time with a high overshoot, little steady state error, and some RMSE target percentage. These findings were due to the real-time analysis and an electrochemical sensor for feedback measurement. Following the PI controller, phase-lag, phase-lead, and phase-lead-lag controllers and a cascaded lead controller were designed and tuned using the root locus method in order to meet the desired requirements. Each controller shows its own merits and demerits in terms of different time domain specifications as shown in Table 4. The gain k is the same for all controllers, which is $k = 500$ except for the PI controller and phase-lag controller. For the PI controller, a much higher gain of $K_p = 4.5 \times 10^6$ is used, making it more vulnerable to noise, when used in real-time analysis. For the phase-lag controller, a gain of $k = 30$ is used, which is essential in order to meet the desired steady state requirement. By using a cascaded lead controller, due to the increased centroid movement, the closed-loop poles of the system move further to the left half plane in the Laplace domain, providing a more quicker response as required. The cascaded lead controller surpasses all the other control techniques, most significantly with a lower gain value of $k = 500$. By employing such technique, the cascaded lead controller with a lower gain value provides relatively better results and response time than the PI controller with a much higher gain value, asserting cascaded lead controller as the most consummate technique.

The comparative analysis of the closed-loop results along with the time domain characteristics illustrated in Table 4 evidently demonstrates and validates the enhanced efficacy of a cascaded lead controller in a closed-loop drug infusion system.

6. Conclusion

Targeting and maintaining the drug concentration level are indispensable in human anatomy and hold central importance as an application of control technology in biomedical engineering. For a closed-loop drug infusion system, simulation of five different controllers has been demonstrated using MATLAB, which shows encouraging results for the delivery of propofol. For faster and stable response of the drug infusion system, comparative analysis for abovementioned controllers has been performed and analyzed. Following the simulation analysis and the results obtained, the cascaded

lead controller and PI controller show the finest results with the cascaded lead controller showing relatively better results than all the other control techniques. The assertive results provide a key platform to implement this model in real time for automatic drug delivery. Such quintessential paradigm in the domain of biomedical control jargon would lead to faster response induction and reduction of clinical workload in the field of total intravenous anesthesia.

Conflicts of Interest

The authors of this manuscript declare that there is no conflict of interest regarding the publication of this paper.

References

- [1] I. Smith and P. F. White, "Types of intravenous anaesthesia," in *Total Intravenous Anaesthesia*, p. 2224, BMJ Publishing Group, London, U.K., 1998.
- [2] I. Smith and P. F. White, "Intravenous anaesthesia delivery and monitoring systems," in *Total Intravenous Anaesthesia*, p. 98127, BMJ Publishing Group, London, U.K., 1998.
- [3] E. Krger-Thiemer, "Continuous intravenous infusion and multicompartment accumulation," *European Journal of Pharmacology*, vol. 4, no. 3, pp. 317–324, 1968.
- [4] S. Syaie, M. A. Rami, and F. Tadeo, "Positive infusion of propofol drug during induction," in *2010 IEEE International conference on industrial engineering and engineering management*, pp. 325–328, Macao, China, December 7–10, 2010.
- [5] A. Simalatsar, M. Guidi, and T. Buclin, "Cascaded PID controller for anaesthesia delivery," in *2016 38th Annual International Conference of the IEEE Engineering in Medicine and Biology Society (EMBC)*, pp. 533–536, IEEE, Orlando, FL, USA, August 16, 2016.
- [6] B. Marsh, M. White, N. Morton, and G. N. Kenny, "Pharmacokinetic model driven infusion of propofol in children," *British Journal of Anaesthesia*, vol. 67, pp. 41–48, 1991.
- [7] T. W. Schnider, C. F. Minto, P. L. Gambus et al., "The influence of method of administration and covariates on the pharmacokinetics of propofol in adult volunteers," *Anesthesiology*, vol. 88, no. 5, pp. 1170–1182, 1998.
- [8] H. Y. Horng, "Lead-lag compensator design based on greedy particle swarm optimization," in *2013 International Symposium on Next-Generation Electronics (ISNE)*, pp. 579–581, Kaohsiung, Taiwan, 25–26 Feb. 2013.
- [9] S. Schaller, J. Lippert, L. Schaupp, T. Pieber, A. Schuppert, and T. Eissing, "Robust PBPk/PD-based model predictive control of blood glucose," *IEEE Transactions on Biomedical Engineering*, vol. 63, no. 7, pp. 1492–1504, 2016.

- [10] I. Kaya, N. Tan, and D. P. Atherton, "Simple procedure for improving performance of pid controllers," in *Proceedings of 2003 IEEE Conference on Control Application, 2003 (CCA 2003)*, vol. 2, pp. 882–885, Istanbul, Turkey, 25–25 June 2003.
- [11] Y. Li, K. H. Ang, and G. Chong, "PID control system analysis and design," *IEEE Control Systems*, vol. 26, no. 1, pp. 32–41, 2006.
- [12] A. S. Hodel and C. E. Hall, "Variable-structure PID control to prevent integrator windup," *IEEE Transactions on Industrial Electronics*, vol. 48, no. 2, pp. 442–451, 2001.
- [13] R. J. Mantz and H. D. Battista, "Comments on variable-structure PID control to prevent integrator windup," *IEEE Transactions on Industrial Electronics*, vol. 51, no. 3, pp. 736–738, 2004.
- [14] H. Y. Horng, "Lead-lag compensator design based on genetic algorithms," in *2012 Conference on Technologies and Applications of Artificial Intelligence (TAAI)*, pp. 80–85, Tainan, Taiwan, 16–18 Nov. 2012.
- [15] P. D. Rohitha, S. Senadheera, and J. K. Pieper, "Fully automated PID and lead/lag compensator design tool for industrial use," in *Proceedings of 2005 IEEE Conference on Control Applications, 2005 (CCA 2005)*, pp. 1009–1014, IEEE, Toronto, Ontario, Canada, 28–31 Aug. 2005.
- [16] Y. Chen, "Replacing a PID controller by a lat-lead compensator for a robot-a frequency-response approach," *IEEE Transactions on Robotics and Automation*, vol. 5, no. 2, pp. 174–182, 1989.
- [17] R. Zanasi and S. Cuoghi, "Design of lead-lag compensators for robust control," in *2011 9th IEEE International Conference on Control and Automation (ICCA)*, pp. 106–111, IEEE, Santiago, Chile, 19–21 Dec. 2011.
- [18] F. Y. Wang and Y. Huang, "A non-trial and-error method for phase-lead and phase-lag compensator design," *IEEE Transactions on Automatic Control*, vol. 22, 2001.
- [19] N. Tan, "Computation of stabilizing lag/lead controller parameters," *Computers and Electrical Engineering*, vol. 29, pp. 835–849, 2003.
- [20] W. C. Messner, M. D. Bedillion, L. Xia, and D. C. Karns, "Lead and lag compensators with complex poles and zeros: design formulas for modeling and loop shaping," *IEEE Control Systems Magazine*, vol. 27, no. 1, pp. 44–54, 2007.
- [21] S. S. Flores, A. M. Valle, and B. A. Castillejos, "Geometric design of lead/lag compensators meeting a Hinf specification," in *2007 4th International Conference on Electrical and Electronics Engineering*, Mexico City, Mexico, September 5–7, 2007.
- [22] R. Zanasi, S. Cuoghi, and L. Ntogramatzidis, "Analytical and graphical design of lead-lag compensators," *International Journal of Control*, vol. 84, pp. 1830–1846, 2011.
- [23] K. Ogata, *Modern Control Engineering*, Prentice-Hall, Englewood Cliffs, NJ, USA, 3rd edition, 1997.
- [24] J. Abdul Jaleel and N. Thanvy, "A comparative study between PI, PD, PID and lead-lag controller for power system stabilizer," in *2013 International Conference on Circuits, Power and Computing Technologies (ICCPCT)*, pp. 456–460, Nagercoil, India, 20–21 March 2013.
- [25] A. Dass and S. K. Jha, "A comparative study of lead, lag, lead-lag and robust controllers for a position control system," in *2014 International Conference on Reliability Optimization and Information Technology (ICROIT)*, pp. 520–523, Faridabad, India, 6–8 Feb. 2014.
- [26] G. W. Evans, "Bringing root locus to the classroom," *IEEE Control Systems*, vol. 24, pp. 674–81, 2004.
- [27] W. R. Evans, "Control system synthesis by root locus method," *Transactions of the American Institute of Electrical Engineers*, vol. 69, pp. 66–69, 1950.
- [28] T. B. Sekara and M. R. Rapai, "A revision of root locus method with applications," *Journal of Process Control*, vol. 34, pp. 26–34, 2015.
- [29] R. Goswami, S. Sanyal, and A. N. Sanyal, "Compensator design for helicopter stabilization," *Procedia Technology*, vol. 4, pp. 74–81, 2012.
- [30] D. M. Sajnekar, S. B. Deshpande, and R. M. Moharil, "Efficient PID controller tuning method selection to be used in excitation system of brushless synchronous generator," in *2016 International Conference on Computation of Power, Energy Information and Communication (ICCPEIC)*, pp. 413–418, IEEE, Chennai, India, 20–21 April 2016.
- [31] C. P. Tan, K. S. Teoh, and L. J. N. Jones, "A review of Matlabs SISOTOOL; features and contributions to control education," *IFAC Proceedings Volumes*, vol. 41, no. 2, pp. 8473–8474, 2008.
- [32] M. H. Myers, Y. Li, F. Kivlehan, E. Lindner, and E. Chaum, "A feedback control approach to organic drug infusions using electrochemical measurement," *IEEE Transactions on Biomedical Engineering*, vol. 63, pp. 506–511, 2016.
- [33] B. C. Kuo, *Automatic Control Systems*, Prentice-Hall International, London, England, 9th edition, 1962.
- [34] M. C. M. Teixeira, "Direct expressions for Ogata's lead-lag design method using root locus," *IEEE Transactions on Education*, vol. 37, no. 1, pp. 63–64, 1994.
- [35] G. F. Franklin, *Feedback Control of Dynamic Systems*, Addison-Wesley Longman Publishing Co., Inc., Boston, MA, USA, 2nd edition, 1993.
- [36] N. S. Nise, *Control System Engineering*, John Wiley and Sons Inc., New York, 2011.



Hindawi

Submit your manuscripts at
<https://www.hindawi.com>

